Nonlinear absorption properties of the charge states of nitrogen-vacancy centers in nanodiamonds

Ivaylo P. Ivanov, Xiangping Li, Philip R. Dolan, and Min Gu*

Centre for Micro-Photonics, Faculty of Engineering and Industrial Sciences, Swinburne University of Technology, P.O. Box 218, Hawthorn, Victoria 3122, Australia

**Corresponding author: mgu@swin.edu.au*

Received February 20, 2013; revised March 19, 2013; accepted March 19, 2013; posted March 20, 2013 (Doc. ID 185560); published April 15, 2013

We have conducted a study on the nonlinear absorption properties of nitrogen-vacancy color centers in processed nanodiamonds. Their two-photon (2P) spectra disclose distinguishable features for the two charge states in which the center exists. The 2P absorption cross section is found to be between 0.1 and 0.5 GM in the wavelength range between 800 and 1040 nm. In addition, the center demonstrates the feature of strong 2P absorption for its neutral charge state below 1000 nm excitation wavelength and predominant 2P absorption by the negative charge state above this wavelength. © 2013 Optical Society of America

OCIS codes: (160.2540) Fluorescent and luminescent materials; (160.4236) Nanomaterials; (190.4180) Multiphoton processes.

http://dx.doi.org/10.1364/OL.38.001358

Recently, nitrogen-vacancy (NV) color centers in diamond have attracted intense research interest and hold great potential in a variety of applications owing to their unique optical and spin properties. A high quantum yield, together with the considerable photostability, exhibiting neither bleaching nor blinking [1,2], make NV centers excellent candidates in bioimaging as fluorescent markers [3]. They exist in two distinct charge states—neutral (NV^0) and negative (NV^-) with discernible spin and optical properties. The negative charge state exhibits a strong dipole-allowed optical transition enabling optically detected magnetic resonance of single electron spins [4]. The long coherence time and outstanding magnetic field sensitivity of NV centers have facilitated magneto-optical imaging with a spatial resolution of 20 nm [5]. In addition, NV centers are considered good candidates for quantum computation [6] and for demonstrating various super-resolution imaging techniques [5,7].

Reversible conversion between the two charge states has been observed when they are exposed to intense irradiation at a number of excitation wavelengths [8]. Windows for selective excitation of either charge state have been identified by exploring their photoluminescence spectra under single-photon (1P) excitation [9]. However, two-photon (2P) excitation of NV centers has been observed only at the excitation wavelengths of 875 and 1064 nm [10,11]. More detailed studies concerning the nonlinear absorption properties and the nature of the charge state transitions under 2P excitation could lead to greater control over the charge state of the NV center and have not yet been carried out.

In this Letter, we concentrate on the studies of single NV centers in nanodiamonds making use of photoluminescence imaging and spectroscopy as well as autocorrelation techniques. This defect is able to switch between both NV^0 and NV^- via photoionization processes and electron trapping. A distinguishable feature of their 2P fluorescence spectra reveals selective excitation windows for either charge state, as illustrated in Fig. 1(a). NV^0 demonstrates dominant 2P absorption for the excitation wavelength from 800 to 1000 nm, switching to NV^- when the excitation is above 1000 nm.

For this set of experiments an unprocessed suspension of high pressure high temperature nanodiamonds, nominally 100 nm in size was used. The nanodiamonds were further diluted in deionized water and centrifuged for 13 min at a rate of 14,000 rpm. This approach preferentially removed larger particles from the suspension and increases the proportion of nanodiamonds containing single NV centers. In addition, this process improves the fluorescence intensity of the sample by eliminating other undesired impurities. Afterward, ultrasound was applied for 10 min to break up agglomerations in the sample. Borosilicate cover slips marked with registration grids were used as the substrate. The final diamond size was measured with an atomic force microscope (AFM) as (60 ± 20) nm as shown in Fig. 1(b). A 1 μm × 1 μm 2P image is shown in the inset. Finally, the solution was drop cast onto the substrates and dried at room temperature.

The nonlinear properties of NV centers were studied with a scanning confocal microscope. A femtosecond laser beam with a repetition rate of 82 MHz, a pulse width of 100 fs and a spectral width of 10 nm (Mai Tai DeepSee) was employed as the 2P excitation source focused by an oil immersion objective lens with a numerical aperture of

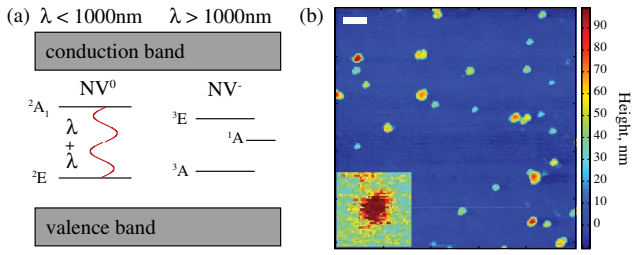

Fig. 1. (a) Charge states excited differently by radiation with wavelengths below and above 1000 nm. (b) AFM image of the sample with a scale bar 1 μm. Inset: 1 μm × 1 μm 2P image of a single emitter.

 © 2013 Optical Society of America

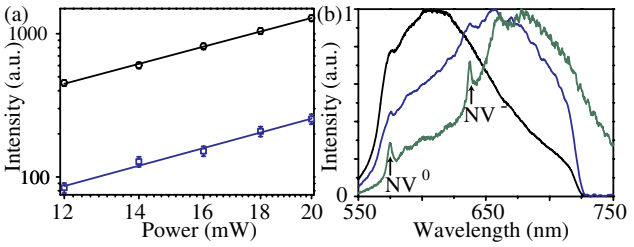

Fig. 2. (a) Logarithmic dependence with slopes of (2.07 ± 0.04) at 800 nm (black line) and (2.12 ± 0.13) at 1000 nm (blue line) of the detected signal versus the input power. (b) Comparison between 2P spectra acquired at 800 nm (black curve), 1040 nm (blue curve) excitation wavelength, and a 1P spectrum with 532 nm (green curve).

1.4. Fluorescence was collected through the same objective and detected by either a spectrograph or a single photon avalanche photodiode (SPAD). The residual laser beam was filtered out by a short pass filter cutting off at 720 nm. Figure 2(a) shows typical examples of fluorescence intensity as a function of the excitation power at wavelengths 800 and 1000 nm plotted in black and blue, respectively. These have been measured by using a 6 mm ∅ excitation laser beam with the power range corresponding to 23.7–45.3 MW/cm^2 in the focal plane. The slopes of approximately 2 on a logarithmic scale unambiguously confirm the 2P excitation nature of the observed nonlinear fluorescence.

Figure 2(b) shows emission spectra obtained at different excitation wavelengths. From the emission spectrum acquired by 1P excitation at the wavelength of 532 nm (green curve), the zero-phonon lines (ZPLs) for NV^- at 638 nm, and NV^0 at 575 nm are distinguishable features indicating the coexistence of the two charge states. The spectrum obtained with excitation at the wavelength of 800 nm (black curve) is blue-shifted compared with that obtained by 1P excitation and the ZPL of NV^- is indiscernible. This result indicates a possible dominant excitation of NV^0 through its phonon sideband (PSB). As the excitation wavelength is increased to 1040 nm (blue curve), the peak of the spectrum noticeably red shifts, and begins to resemble the 1P emission spectrum. This is attributed to more effective absorption by the NV^- PSB at longer wavelengths and is consistent with recent photoluminescence excitation measurements [9]. Under 532 nm 1P excitation, the ZPLs are sharper and more pronounced and are both clearly in evidence. The reduced visibility of ZPLs in the 2P excitation spectra may be explained by the considerably higher excitation intensities required for the nonlinear process. The higher intensities are likely to contribute to much stronger local heating effects which may thermally broaden the ZPLs.

From the acquired fluorescence signal, it is possible to estimate the 2P absorption cross section of an NV center as [12]:

$$\sigma_2 \sim \frac{F}{\eta \phi N I^2}, \tag{1}$$

where F is the fluorescence counts acquired by the SPAD, η is the fluorescence quantum yield, ϕ is the collection efficiency of the confocal system, and N is the number of emitters inside the focal volume and I is the incident intensity.

To determine the number of NV centers inside the focal spot, a Hanbury Brown–Twiss setup was used [13]. Figure 3(a) presents a second-order autocorrelation dependence by 1P excitation at the wavelength of 532 nm. The normalized second-order autocorrelation function at the zero delay is given as [14]:

$$g^{(2)}(0) = 1 - \frac{1}{N}. \tag{2}$$

At the point of zero delay, the value of the second-order autocorrelation function approaches zero, which unambiguously indicates the presence of a single emitter in the focal region.

The system collection efficiency of (0.0007 ± 0.0001) is estimated for our experimental configuration and a quantum yield of the NV center as 0.7 is taken [15] to calculate the cross sections for the single NV center examined and these are plotted in Fig. 3(b) as blue squares. Their values vary between 0.1 and 0.5 GM and are in good agreement with other results obtained by the 2P excitation of NV centers in a bulk diamond {(0.45 ± 0.23) GM at 1064 nm [10]}. This is three orders of magnitude smaller than that of typical CdS quantum dots [12].

For a comparison, we performed another set of measurements on the 2P absorption cross sections of NV centers in agglomerations. By comparing the fluorescence counts from a single emitter to the aggregation we estimated the number of emitters in the focal spot of the aggregated sample to be (12101 ± 308). For this purpose a correction factor of 1.8 due to the random dipole orientation under excitation by linearly polarized light was adopted by following the previous theoretical estimation by Monte Carlo simulations [16]. The estimated 2P absorption cross sections per NV center in the agglomeration are shown in Fig. 3(b) as red circles. Their values are in reasonable agreement with the results obtained from single NV centers over the investigated range. These results may imply that the immediate environment of NV centers has less effect on the 2P excitation properties of NV centers.

There is considerable variation in the cross-section values across the spectrum with several local maxima at 860, 900, and 980 nm. The black curve represents an

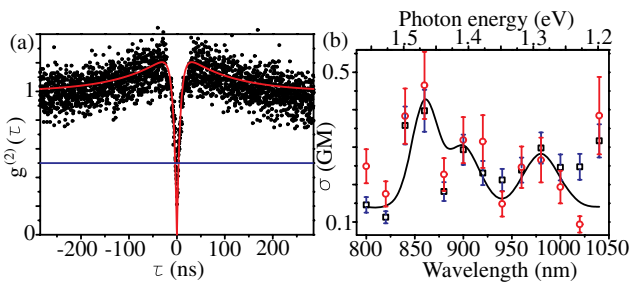

Fig. 3. (a) Second-order autocorrelation function versus the time delay as evidence of single center emission. (b) 2P absorption cross sections of NV centers obtained by excitation of single (blue squares) and aggregated (red circles) NV centers. An approximation of the dependence based on Gaussian curves is plotted in black.

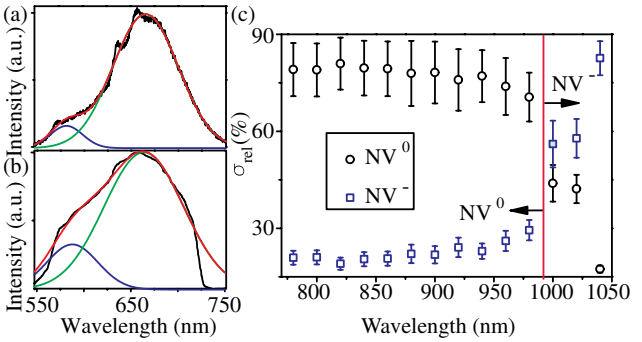

Fig. 4. (a) 1P spectrum at 532 nm and (b) 2P spectrum at 1040 nm fitted as a sum of two Gaussian functions responsible for the absorption of the two charge states. (c) Relative 2P absorption cross sections for the two feasible charge states the center exists.

approximation of the experimental data as a sum of Gaussian functions. This structure may be explained by variations in the coupling strength of the electronic transition to local vibronic modes. The differences in energy (64 and 113 meV) between these peaks are close to the energies predicted by various *ab initio* studies [17,18].

As suggested by the variation in spectra shown in Fig. 2(b), the proportion of the total luminescence contributed by the NV^0 and NV^- shifts as the excitation wavelength is increased. By using the established approximation of modeling the emission characteristics of both NV^0 and NV^- as Gaussian functions [19] we can quantitatively estimate the relative contribution of the two charge states to the cross-sectional area. To do this we first fit two Gaussian functions to the emission spectrum obtained with the 532 nm excitation, shown in Fig. 4(a). This provides a benchmark for the fitting parameters to be used in fitting the 2P emission spectra. An example of the fitting performed with the excitation wavelength of 1040 nm is plotted in Fig. 4(b). The fitting procedure consistently reproduced the acquired spectra, and achieved errors of less than 8% for the unfiltered spectral region. By taking the ratio of the fitted Gaussian plots we arrive at the percentage contribution to the overall cross section of absorption, shown in Fig. 4(c).

From this data we see that at wavelengths around 1000 nm the two states absorb equally. Above this wavelength NV^- dominates the absorption whilst below this wavelength NV^0 contributes mostly to the measured emission spectrum. We found that the 2P absorption cross-sectional area of NV^0 was 3.75 times larger than the NV^- area at 800 nm, whilst the NV^- 2P absorption cross-sectional area becomes 4.75 times larger at 1040 nm. These results are in good agreement with the respective regions of single photon absorption, which start around 400 nm up to the ZPL at 575 nm for NV^0 and around 450 nm up to the NV^- ZPL at 638 nm [8]. The spectral extent of the 2P phonon assisted absorption is twice that of the 1P absorption, as expected for centers with no central symmetry.

In conclusion, the nonlinear excitation properties of NV centers in processed nanodiamonds have been systematically studied by using the 2P fluorescence method. 2P absorption cross sections between 0.1 and 0.5 GM are found for excitation wavelengths from 800 to 1040 nm for both single and agglomerated samples. A selective nonlinear excitation window between 800 and 1000 nm for the neutral charge state is identified. Above the excitation wavelength of 1000 nm 2P absorption by the negatively charged state dominates. These results are of great importance, opening a new window for a better control of the charge states of NV centers with desired spin properties by the selective excitation at infrared wavelengths.

This work was supported by the Australian Research Council Laureate Fellowship project (FL100100099).

References

1. A. Gruber, A. Drabenstedt, C. Tietz, L. Fleury, J. Wrachtrup, and C. von Borczyskowski, Science **276**, 2012 (1997).
2. S. Kuhn, C. Hettich, C. Schmitt, J. P. H. Poizat, and V. Sandoghdar, J. Microsc. **202**, 2 (2001).
3. Y. Y. Hui, C.-L. Cheng, and H.-C. Chang, J. Phys. D **43**, 374021 (2010).
4. N. Diep Lai, D. Zheng, F. Treussart, and J.-F. Roch, Adv. Nat. Sci. Nanosci. Nanotechnol. **1**, 015014 (2010).
5. G. Balasubramanian, I. Y. Chan, R. Kolesov, M. Al-Hmoud, J. Tisler, C. Shin, C. Kim, A. Wojcik, P. R. Hemmer, A. Krueger, T. Hanke, A. Leitenstorfer, R. Bratschitsch, F. Jelezko, and J. Wrachtrup, Nature **455**, 648 (2008).
6. P. Neumann, R. Kolesov, B. Naydenov, J. Beck, F. Rempp, M. Steiner, V. Jacques, G. Balasubramanian, M. L. Markham, D. J. Twitchen, S. Pezzagna, J. Meijer, J. Twamley, F. Jelezko, and J. Wrachtrup, Nat. Phys. **6**, 249 (2010).
7. S. Castelletto, X. Li, and M. Gu, J. Nanophoton. **1**, 139153 (2012).
8. K. Beha, A. Batalov, N. B. Manson, R. Bratschitsch, and A. Leitenstorfer, Phys. Rev. Lett. **109**, 097404 (2012).
9. G. W. N. Aslam, P. Neumann, F. Jelezko, and J. Wrachtrup, New J. Phys. **15**, 013064 (2013).
10. T. L. Wee, Y. K. Tzeng, C. C. Han, H. C. Chang, W. Fann, J. H. Hsu, K. M. Chen, and Y. C. Yull, J. Phys. Chem. A **111**, 9379 (2007).
11. Y. Y. Hui, B. Zhang, Y.-C. Chang, C.-C. Chang, H.-C. Chang, J.-H. Hsu, K. Chang, and F.-H. Chang, Opt. Express **18**, 5896 (2010).
12. X. Li, J. van Embden, J. W. M. Chon, and M. Gu, Appl. Phys. Lett. **94**, 103117 (2009).
13. L. Dai and L. Kwek, Phys. Rev. Lett. **108**, 066803 (2012).
14. H. Paul, Rev. Mod. Phys. **54**, 1061 (1982).
15. G. Waldherr, J. Beck, M. Steiner, P. Neumann, A. Gali, T. Frauenheim, F. Jelezko, and J. Wrachtrup, Phys. Rev. Lett. **106**, 157601 (2011).
16. Y. Y. Hui, Y.-R. Chang, T.-S. Lim, H.-Y. Lee, W. Fann, and H.-C. Chang, Appl. Phys. Lett. **94**, 013104 (2009).
17. A. Gali, Phys. Rev. B **79**, 235210 (2009).
18. J. Zhang, C.-Z. Wang, Z. Zhu, and V. Dobrovitski, Phys. Rev. B **84**, 035211 (2011).
19. M. S. Haque, H. A. Naseem, J. L. Shultz, W. D. Brown, S. Lal, and S. Gangopadhyay, J. Appl. Phys. **83**, 4421 (1998).